Electronic Supplementary Material (ESI) for Lab on a Chip

Electronic Supplementary Information for:

Microfluidic genome-wide profiling of intrinsic electrical properties in *Saccharomyces cerevisiae*

Michael D. Vahey[1]*, Laia Quiros Pesudo[2], J. Peter Svensson[3], Leona D. Samson[2], Joel Voldman[1]

[1] Department of Electrical Engineering and Computer Science, Massachusetts Institute of Technology, Cambridge, MA 02139

[2] Biological Engineering Department, Center for Environmental Health Sciences, Biology Department, Koch Institute for Integrative Cancer Research, Massachusetts Institute of Technology, Cambridge, MA 02139

[3] Department of Biosciences and Nutrition, Karolinska Institutet, 14183 Huddinge, Sweden

*Currently at the Department of Bioengineering, University of California Berkeley, Berkeley, CA 94720

ESI Methods

Cell culture and sample preparation for sorting

For pairwise comparisons of mutant and wildtype cells, strains were streaked on YPD + agar plates and cultured until ~1mm diameter single colonies could be selected and transferred to liquid medium. As in the pooled experiments, cells were grown to a density of ~3×10^8 cells/ml prior to the separation. Unlike pooled experiments, fluorescent labels were applied (SYTO 9 and SYTO 64, 5μM with a 10 minute incubation at room temperature) to visually discriminate between the two different strains. Immediately after staining, cells were washed 3× in separation medium, re-suspended at a concentration of ~$2\text{-}5\times10^7$ cells/ml, and characterized in the IDS device. Sample preparation and fluorescent labeling was observed to not impact cell viability (determined by staining with propidium iodide) over time courses significantly longer than those required for the IDS strain comparisons (~3 hours vs. ~30 minutes).

Operating conditions for pooled and pairwise separations

We performed separations of the pooled deletion collections under two sets of operating conditions, with two independent replicates under each condition. The different operating conditions allowed us to probe different cellular compartments, as described in the main article. At lower electric field frequencies (< 1 MHz), the screen is primarily sensitive to the electrical properties of the cell envelope, whereas at higher electric field frequencies (>1 MHz), the sensitivity shifts to the interior of the cell. Because isodielectric separation requires that cells be suspended in a medium in which they have negative polarizability at the frequency of interest, the range of electrical conductivities used for these separations is different. At a frequency of 300 kHz, the conductivity range spans from 0.065 S/m to 0.01 S/m; at 10 MHz, the range is from 0.35 S/m to 0.12 S/m. The electrical conductivity of the medium is adjusted through the addition of phosphate buffered saline, in addition to 0.5% bovine serum albumin to minimize non-specific adhesion of cells to the surface of the device during separations.

Device architecture and operating conditions differ slightly for high frequency and low frequency experiments. In addition to differences in the electric field frequency used, a higher impedance device is used for experiments at 10 MHz, with one set of electrodes in parallel, as opposed to four sets in parallel for the lower frequency experiments. This is to compensate for the ~5× higher conductivity required at this frequency. In all cases, the operating voltage is maintained at 10 V_{pp} across an electrode spacing of 15μm and the channel geometry is identical (2mm width × 20μm depth × 30mm length). Monitoring cell uptake of propidium iodide on interdigitated electrode arrays for both wildtype and mutant (rim101Δ) strains under comparable electric field conditions suggested that cell viability should not be affected by the transient exposure (~10-15s) to the electric field experienced by cells during separation.

Distributions of average conductivity across deletion strains

An important constraint for intrinsic separation methods is the relative magnitude of specific versus non-specific variation in the population being analyzed. In this work, we assess this constraint by comparing the distribution of average conductivities *across* the deletion strains (*i.e.* the specific variation) to the distribution of conductivities *within* a particular strain (*i.e.* the non-specific variation).

To determine the approximate distribution of effective conductivities for each strain, we first reconstruct the distribution of each strain across the four sorted fractions. We do this by

constraining the composite frequency of each strain collected in all four outlets to match the frequency of each strain in the original pool:

$$p_1 f_1 + p_2 f_2 + p_3 f_3 + p_4 f_4 = f_0$$

Here, p_i gives the fraction of total cells collected in outlet i, so that $\Sigma p_i = 1$. Because this problem is over-determined, we minimize the error between f_0 and the weighted sum over the four outlets summed over all N strains. The distribution of the n^{th} strain across the four outlets (i = 1,2,3,4) is then $p_i f_i^n / f_0^n$. Although the sum over this distribution would ideally equal one for all strains, discrepancies are introduced in solving the over-constrained system. To eliminate this, we renormalize each of the distributions.

Combining the spatial distribution with the conductivity profile and models for force balance, we can determine the distribution of effective conductivity as described previously (19). This generates the distributions in Figure 2 in the main article. To approximate the standard deviation in effective conductivity for each strain, we scale the standard deviation in the spatial position of each strain by the gradient in conductivity. ESI Datasets S1 and S2 list the average and spread of effective conductivity for each strain in screens performed at 300 kHz and 10 MHz, respectively.

Pairwise comparison of strains and false-positive rate

To test strains identified in the pooled screens as having particularly high enrichments at increased or decreased conductivities, we compare them directly to the parental strain from which they were derived (BY4741). Cell culture, sample preparation, and device operation are described in Materials and Methods. We image the fluorescently labeled cells as they approach the outlet of the device, recording ~10s of video (capturing ~10^4 cells) for each fluorescent channel (FITC and TRITC filter sets, 5× magnification) in immediate succession. We high pass filter the recorded video and average across each frame to obtain a composite image of the cell trajectories, which we further average along the channel length to obtain a one-dimensional profile. Normalizing the profile for both the deletion and wildtype strains gives approximate probability distributions $p_\Delta(x)$ and $p_{\text{wt}}(x)$ for a mutant or wildtype cell passing through the electrode barrier at position x. This process is repeated across different electric field frequencies (100-500 kHz for validation of results from the pooled screens at 300 kHz).

The mean of each distribution is given from the first moment, $\langle x \rangle = \int_0^w x p(x) dx$, where w is the width of the channel. ESI Figure S1 plots $\langle x \rangle_\Delta - \langle x \rangle_{wt}$ for 29 strains we have compared to wildtype in this way. Each bar represents the average shift in distributions (± s.d.) for frequencies <300 kHz. We choose to focus on lower frequencies because we find that these conditions are often more sensitive than the higher frequencies in detecting differences in distributions (i.e. strains that cannot easily be distinguished at 500 kHz are sometimes become separated as the frequency is decreased). As a negative control, we follow this same procedure using differently labeled wildtype cells, using this as a baseline for determining which deletion strains appear significantly different from wildtype (two-sample t-test with a cutoff p-value of 0.05). Based upon this metric, 3 of the 29 strains are scored as false positives: *ldb18*Δ (P = 0.157), *pef1*Δ (P = 0.104), and *swi6*Δ (P = 0.058).

For each deletion strain / wildtype comparison, we image fluorescently labeled cells for the purposes of general morphological comparison (Fig. S1*b*). Of the strains analyzed, 12 were associated with altered morphology in homozygous diploid strains by Giaever et al. (16): *dia4* (elongate 3), *kel1* (elongate 3), *cdc50* (football 2), *sit4* (clumpy 2), *pef1* (small 2), *swi6* (elongate 3), *swi3* (chain 3), *alg8* (round 3), *ssn3* (football 3), *sfl1* (round 2, clumpy 2), *erd1* (round3, clumpy 3), and *ace2* (clumpy 3). These scores are in agreement with our observations for haploid deletion strains. Of the remaining strains, 14 are categorized as "wildtype" (in agreement with our observations) and three (*chs1*, *rcy1*, and *hda1*) as "not determined"; of the strains not characterized, only *hda1* appears morphologically distinct (larger and more elongate than wildtype cells).

Comparison of electrical properties to other phenotypic data

Morphology. Data for the morphology of deletion strains is taken from reference (16), where homozygous diploid strains were scored on a scale from 1-4 with 1 representing wildtype morphology and 4 representing the strongest difference from wildtype. For comparison to the electrical profile, we looked for enriched morphological categories in strains whose log ratio y was >2 s.d. from the mean (i.e. either increased or decreased effective conductivity) under one or more of the screening conditions. Any strain receiving a score of ≥2 in the morphology screen was included as morphologically distinct. The results of this analysis are shown in ESI Figure S2 for categories that have significant enrichment ($P < 0.01$). In this figure, the numbers associated with each morphological category exclude 788 strains for which electrical data was not available for both of the electric field frequencies. Here and in all other cases where we are filtering strains identified in the electrical profile through other datasets, P-values are calculated using a hypergeometric distribution to determine the probability of finding a given number of strains common to two datasets, given the overall size and frequency of the characteristics of interest within the respective full datasets.

Figure 4*b* in the main article gives frequencies for each morphological category among strains with different electrical properties. For strains in which the effective conductivity is increased ($y > 2$ s.d) at either frequency, there is significant enrichment of elongate and football morphologies, whereas among strains with decreased effective conductivities ($y < -2$ s.d) there is significant enrichment of "small" and "round" morphologies.

Fitness and chemical genomic profiling. For comparison to fitness and chemical genomic profiling, we use data from Deutschbauer *et al*. (21) and Hillenmeyer *et al*. (4). For fitness comparisons (Figure 4*a* in the main article), we consider a (homozygous) deletion strain to exhibit a growth defect if it's growth is < 0.9 that of wildtype. Figure 4*a* in the main article counts only those strains for which both electrical and fitness profiling data was available (4382 strains).

For chemical genomic profiling data, we searched for environmental conditions in which electrically distinct strains (log ratio y > 3s.d. from mean) were enriched for sensitivity or resistance (fitness log ratio > 3s.d. from the mean). Among strains with increased cell envelope conductivity, there is significant correlation with salt sensitivity (21% of strains with this electrical phenotype vs. 1.95% overall, for 700uM NaCl), while among strains with decreased intracellular conductivity, we find significant correlation with sensitivity to nutritional limitations (11% of strains with this electrical phenotype, vs. 1.2% overall sensitivity for cells grown on synthetic complete media). Similar enrichments are observed for cells grown at

different salt concentrations, or in the absence of specific amino acids. *P*-values reported in the main article are determined from a hypergeometric distribution, using the frequency of strains in the electrical profile with a given electrical phenotype and the frequency of strains in the chemical genomic profile exhibiting the target sensitivity or tolerance.

Protein localization and abundance. Protein localization and abundance data is taken from Huh et al. (23) and Ghaemmaghami et al. (24), respectively. We compare strains with log ratios (= y) > 2 s.d. from the mean against 23 different localization categories, a subset of which are plotted in Figure 5*a* in the main article. To determine which localization categories are significantly enriched under different categories among strains with different electrical phenotype, we calculate a P-value based on a hypergeometric distribution using the frequency of strains with the observed electrical properties and the frequency of proteins with a given localization. Categories with $P < 0.01$ are considered substantially enriched, and categories with $P < 0.002$ are considered to be significantly enriched, based on applying the Bonferroni correction for 23 comparisons with an alpha value of ~0.05. ESI Table S1 displays frequencies and P-values for all 23 localization categories for strains with distinct electrical properties. The overall frequency for each localization category refers to the frequency of that category among strains for which we have electrical data.

In the main article, we mention that protein abundance and electrical properties are not strongly correlated. This is illustrated by the scatter plots in ESI Figure S3, from which we calculate Pearson correlation coefficients (= r) of -0.095 and 0.026 between log copy-number and the electrical log-ratio, y, at 300 kHz and 10 MHz, respectively.

Gene Ontology Biological Process terms. Lists of genes associated with each of 44 GO Biological Process slim terms ('complete mapping' approach) were downloaded from the *Saccharomyces cerevisiae* Genome Database for comparison to the strains identified from the electrical profile ($|y| > 2$s.d. from the mean). The significantly enriched categories are determined using a *P*-value cutoff of 0.001 (applying the Bonferroni correction with an alpha value of ~0.05), calculated using a hypergeometric distribution. The enriched categories under this criterion are plotted in Figure 5*b* in the main article; a complete listing of the frequency of different terms within electrically distinct strains and the associated *P*-values is given in ESI Table S2. Specific genes associated with significantly enriched GO Biological Process terms is given in ESI Dataset S3.

Genetic and protein-protein interactions. To determine possible functional relationships between genes whose deletion alters a cell's electrical phenotype, we use data from Costanzo *et al.* (25). Here, functional interactions between genes are categorized as positive or negative, and subjected to different thresholds for significance. We compare our electrical profile to three different categories of genetic interaction data: all interactions (positive and negative) with stringent cutoff, positive interactions only with stringent cutoff, and positive interactions only with intermediate cutoff. We have chosen to emphasize positive interactions so as to focus on genes which may participate in the same pathway(s). Table S3 provides results for the size and connectedness of networks among genes associated with distinct electrical properties.

As discussed in the main article, the electrical phenotypes most significantly enriched for genetic interactions are increased conductivity at 300 kHz, and decreased conductivity at 10 MHz. In addition, strains with decreased conductivity at 300 kHz are also enriched, but to a lesser degree of significance. Strains with increased conductivity at 10 MHz, in contrast, are not

significantly enriched for genetic interactions. To determine the expected number of connections and the significance of enrichments, we define the edge probability for the overall network as:

$$p = \frac{2E}{N(N-1)}$$

where E and N are the number of edges and nodes in the complete network, respectively. For a sub-network consisting of n nodes, the expected number of edges is given by $\langle e \rangle = pn\,(n-1)/2$. Similarly, the P-value for the observed number of edges, e, given a sub-network of n nodes within a larger network of N nodes and E edges, is determined from a hypergeometric distribution. In this calculation, we ignore the specific identities of the n nodes for simplicity. Before applying the electrical profile to these networks, we eliminate genes associated with libraries we did not screen (temperature sensitive mutants and DAmP strains), obtaining the values for N and E given in ESI Table S3. We follow a similar procedure in searching electrically distinct strains for physical (protein-protein) interactions, using data from Krogan *et al.*(27).

We use a similar approach to determine if the n nodes associated with distinct electrical properties are enriched for positive genetic interactions with the external network (containing N-n nodes). Since each of the n nodes in this case can have N-n connections to the external network, the expected number of edges is given by $pn(N\text{-}n)$. Combining these edges with the expected number of edges internal to the sub-network provides an expected number of total edges. Comparing this value with the observed number of edges shows the enrichment in edges for all categories of altered electrical phenotype: 456 edges observed (vs. 280 predicted) for increased conductivity at 300 kHz; 235 edges observed (vs. 124 predicted) for decreased conductivity at 300 kHz; 269 edges observed (vs. 215 predicted) for increased conductivity at 10 MHz; and 612 edges observed (vs. 323 predicted) for decreased conductivity at 10 MHz.

ESI Discussion

Sampling strains during separation

In order to account for each strain in the deletion collection robustly, we require that each strain be sampled during collection at least K times, where K is a number to be specified. If a particular strain occurs in the deletion library with frequency f, the probability density function for the number of times it has been sampled (= k) when N cells have been collected is given by:

$$p[k] = \binom{N}{k} (f)^k (1-f)^{N-k} \approx \frac{1}{\sqrt{2\pi fN}} \exp\left\{ -\frac{(k-fN)^2}{2fN} \right\} \quad \textbf{(1)}$$

The corresponding cumulative distribution function gives the probability that $k > K$, so that the sampling of this strain satisfies our criterion for redundancy. If we require that this criterion be satisfied for each of M total strains and assume the strains are sampled independently, we have:

$$[P(k \geq K)]^M \approx \frac{1}{2^M} \left[1 - \mathrm{erf}\left\{ \frac{(K-fN)}{\sqrt{2fN}} \right\} \right]^M \geq X \quad \textbf{(2)}$$

Here, X ($0 < X < 1$) reflects the desired level of certainty in having sampled each strain at least K times during cell collection. To solve for N, we first define $q \equiv (fN - K)/\sqrt{2fN}$, and use the large x expansion $\mathrm{erf}(x) \sim 1 - \exp(-x^2)/\sqrt{\pi}x$ along with the approximation, valid for large M, $(1+x)^M \sim \exp(Mx)$. This gives:

$$\frac{1}{2^M}[1 + \mathrm{erf}(q)]^M \approx \exp\left\{ -\frac{Me^{-q^2}}{2\sqrt{\pi}q} \right\} \geq X \quad \textbf{(3)}$$

Solving for q involves a transcendental equation, $q = \left[\log\{M/(2\sqrt{\pi}q\log(X^{-1}))\}\right]^{1/2}$. Since the right-hand side is only weakly dependent on q and X, and $M \gg 2\sqrt{\pi}$, an accurate approximation is $q \approx [\log\{M\}]^{1/2}$. Combining this result with the definition of q gives the number of cells N that must be collected to satisfy our requirement:

$$N \approx M\left[K + \log(M) + \sqrt{2K\log(M)} \right] \quad \textbf{(4)}$$

This equation assumes that all strains are present at the same frequency, $1/M$. In the more general case, where each strain may be present in the library at a different frequency (= f_i), we would have $q_i \equiv (f_i N - K)/\sqrt{2f_i N}$ and the number of cells we need to collect would be determined by solving $\sum_{i=1}^{M} \exp(-q_i^2)/2\sqrt{\pi}q_i = \log(1/X)$. If we further assume that the representation of different strains differ significantly (as is the case if the pooled library is grown for several generations), then N will be determined almost entirely by the number and frequency of the slowest growing strain(s). Despite its simplifications, equation (4) provides a reasonable guideline for the number of cells one must collect to sample each of M total strains at least K times. Note that, to leading order, the level of certainty, X, does not matter; this is because equation (2) transitions from 0 to 1 over a very narrow range of N when M is large. Also worth noting is that requiring that all strains be sampled at least K times is not much more stringent than requiring that one particular strain be sampled K times; this effectively increases N by an amount $M\sqrt{2K\log M} \ll MK$.

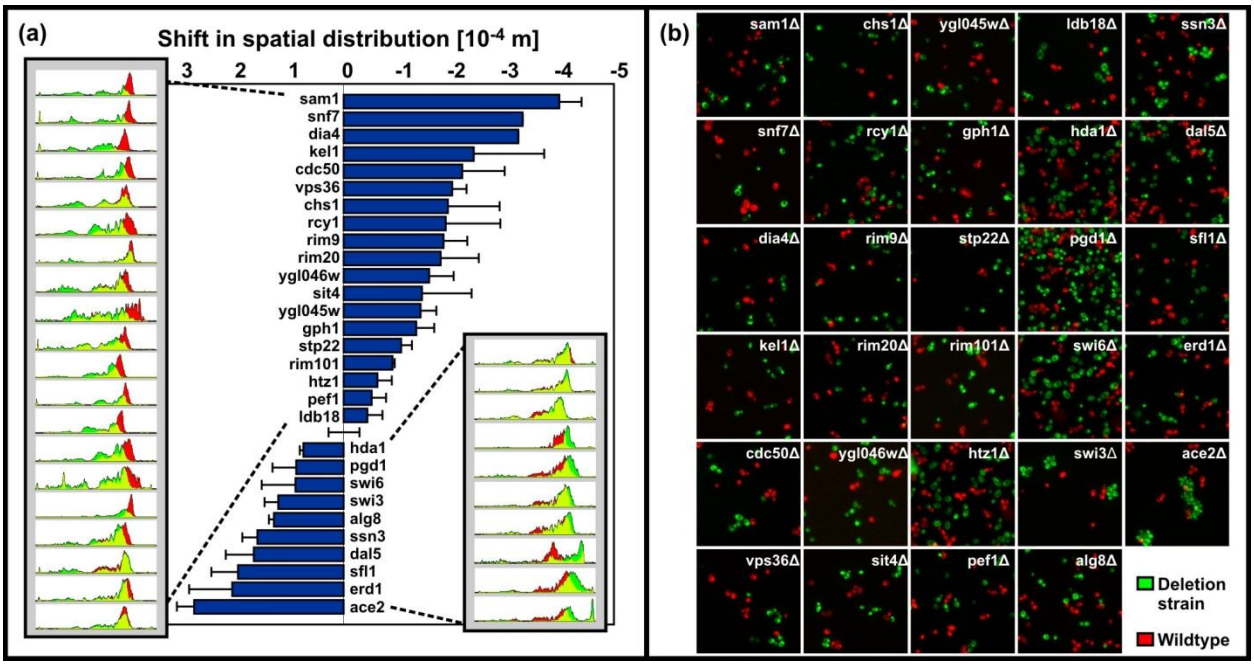

ESI Figure S1

Pairwise comparisons between mutant strains identified as having altered electrical phenotype (shown in green) and wildtype strains (BY4741; shown in red). (*a*) A plot showing how the distributions of mutant strains are shifted relative to the parental wildtype strain. Each bar corresponds to a pairwise comparison between one mutant strain and the parental wildtype strain (BY4741), with the height giving the shift in the mean of the spatial distribution observed during the separation. The accompanying line plots show the spatial distributions of the two strains obtained during separation, with conductivity decreasing from left to right. In these plots, a negative shift in the spatial distribution therefore corresponds to an increase in effective conductivity. (*b*) Fluorescent images of strains analyzed in validating the results of pooled screens.

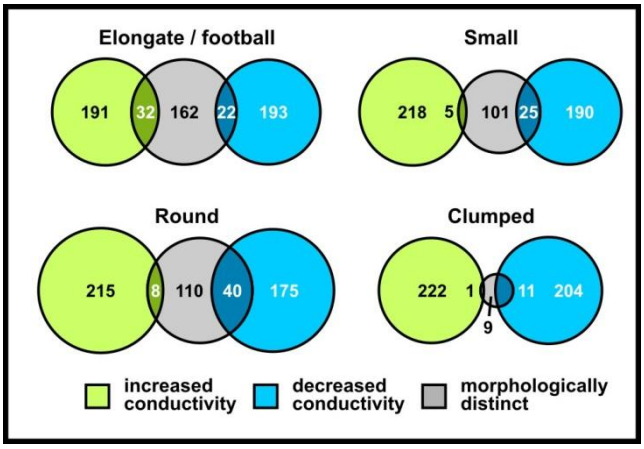

ESI Figure S2

Comparisons between electrical properties and morphological data. Overlap between electrically distinct strains and significantly enriched morphological categories ($P < 0.01$).

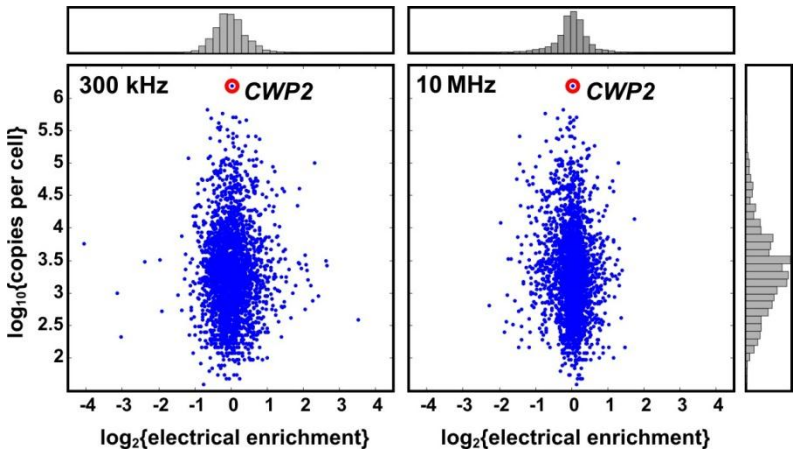

ESI Figure S3

Comparison between the abundance of a protein (copies per cell) and the electrical properties of a strain lacking that protein. The low correlations at both lower and higher electric field frequencies (r = -0.095 and 0.026, respectively) suggests that deletion of high copy number proteins does not typically have an enhanced effect on electrical properties, which are more strongly correlated with protein function than abundance.

Category	Decreased, 10 MHz		Increased, 10 MHz		Decreased, 300 kHz		Increased, 300 kHz		Overall Freq.
	Freq.	$\log_{10}(P)$	Freq.	$\log_{10}(P)$	Freq.	$\log_{10}(P)$	Freq.	$\log_{10}(P)$	
cytoplasm	0.2793	-0.0959	0.3148	-0.3469	0.2241	-0.0286	0.4118	-2.3111	0.3052
nucleus	0.1285	-0.0013	0.2685	-1.226	0.3448	-2.0717	0.2647	-1.2992	0.2031
mitochondrion	0.2067	-5.8813	0.0741	-0.1031	0.0862	-0.196	0.0956	-0.301	0.0919
ER	0.0782	-1.5266	0.0556	-0.4446	0.0517	-0.3114	0.0368	-0.1304	0.045
ambiguous	0.0447	-0.2932	0.0278	-0.0698	0.0862	-1.0136	0.0221	-0.0301	0.043
vacuole	0.0279	-0.1734	0.0278	-0.1759	0.0345	-0.2585	0.0221	-0.0912	0.0314
cell periphery	0.0056	-0.0024	0.037	-0.4431	0.0172	-0.0906	0.0221	-0.1277	0.0281
punctate composite	0.0223	-0.1892	0.0093	-0.0298	0.0172	-0.1137	0.0368	-0.6049	0.0245
bud neck	0.0168	-0.2643	0.0185	-0.2889	0	0	0.0147	-0.1921	0.0158
nucleolus	0.0447	-2.9258	0	0	0.0172	-0.2885	0.0294	-1.0703	0.012
Bud	0.0279	-1.261	0.0093	-0.1423	0.0345	-0.8366	0.0074	-0.0962	0.0116
vacuolar membrane	0.0335	-2.0352	0.0185	-0.5165	0	0	0.0221	-0.7868	0.0103
endosome	0.0112	-0.297	0.0185	-0.5712	0.0172	-0.3729	0.0147	-0.4349	0.0094
nuclear periphery	0.0056	-0.1132	0.0185	-0.6684	0.0345	-1.1037	0.0074	-0.1722	0.008
late Golgi	0.0056	-0.1244	0	0	0.0172	-0.4441	0.0074	-0.1859	0.0076
early Golgi	0.0112	-0.4525	0	0	0.0172	-0.4764	0.0074	-0.2093	0.0069
Golgi	0.0056	-0.1843	0	0	0	0	0.0074	-0.2465	0.0058
Actin	0.0168	-1.1648	0	0	0.0172	-0.5691	0.0074	-0.2801	0.0054
spindle pole	0.0056	-0.2272	0	0	0.0172	-0.6191	0	0	0.0049
peroxisome	0	0	0	0	0	0	0	0	0.0045
lipid particle	0	0	0.0093	-0.4303	0.0345	-1.6095	0	0	0.0042
microtubule	0.0056	-0.3394	0	0	0.0172	-0.7491	0	0	0.0033
ER to Golgi	0	0	0	0	0	0	0	0	0.0002

ESI Table S1.
Frequencies of localization categories for proteins whose deletion substantially changes electrical properties. "Freq." refers to the frequency of each category among strains with a particular electrical phenotype (e.g. decreased conductivity at 10 MHz); the overall frequency is listed in the right-most column.

Category	Decreased, 10MHz		Increased, 10MHz		Decreased, 300kHz		Increased, 300kHz		Overall Freq.
	Freq.	$\log_{10}(P)$	Freq.	$\log_{10}(P)$	Freq.	$\log_{10}(P)$	Freq.	$\log_{10}(P)$	
Transport	0.2011	-1.1245	0.1574	-0.2502	0.1207	-0.0767	0.2059	-1.0733	0.1592
Bio. proc. unknown	0.0168	0	0.1481	-0.1991	0.0345	-0.0003	0.1176	-0.0367	0.1561
RNA met. proc.	0.2346	-4.8427	0.1944	-1.7139	0.3103	-3.9306	0.2059	-2.4569	0.1222
Response to stress	0.095	-0.2888	0.1019	-0.3647	0.069	-0.0932	0.1912	-3.5475	0.0936
Protein mod. proc.	0.1006	-0.6384	0.1019	-0.5455	0.1207	-0.7094	0.0735	-0.1606	0.0832
Transcription	0.1061	-0.8705	0.1574	-2.2475	0.2759	-5.0934	0.1324	-1.6156	0.0812
Response to chem.	0.067	-0.1834	0.1019	-0.8048	0.0862	-0.3843	0.1176	-1.4485	0.0725
Cell cycle	0.067	-0.201	0.1759	-3.762	0.1552	-1.7229	0.1471	-2.9291	0.0711
Translation	0.2402	-11.5794	0.0463	-0.1606	0.0862	-0.6913	0.0809	-0.9319	0.0533
Chromosome org.	0.0503	-0.2098	0.0741	-0.6713	0.069	-0.4351	0.1103	-2.3053	0.0531
DNA met. proc.	0.0447	-0.1312	0.1019	-1.581	0.1034	-1.0852	0.0662	-0.5439	0.0528
Vesicle-med. trans.	0.1006	-2.2308	0.0463	-0.1652	0.0862	-0.7268	0.0956	-1.594	0.0528
Carb met. proc.	0.0503	-0.3513	0.0556	-0.419	0.0517	-0.2969	0.0809	-1.3209	0.0462
Amino acid met. proc.	0.0503	-0.4599	0.037	-0.1681	0.0172	-0.0358	0.0882	-1.9121	0.0424
Mitochon. org.	0.162	-9.8625	0.0463	-0.3221	0.0172	-0.0368	0.0441	-0.2899	0.0419
Membrane org.	0.1173	-5.0078	0.0556	-0.5499	0.0517	-0.3702	0.0956	-2.4617	0.041
Signalling proc.	0.0559	-0.7861	0.0463	-0.3778	0.0345	-0.1757	0.0368	-0.2096	0.0392
Lipid met. proc.	0.0615	-1.5551	0.0278	-0.1669	0.0345	-0.2524	0.0221	-0.0872	0.0321
Metabolite gen.	0.0726	-2.6163	0.037	-0.3928	0.0517	-0.6055	0.0588	-1.314	0.0299
Protein complex biogen.	0.0447	-0.9034	0.0463	-0.7401	0.0345	-0.3208	0.0515	-1.0988	0.0279
Component morph.	0.0391	-0.6594	0.0648	-1.5547	0.0172	-0.0948	0.0441	-0.7679	0.0274
Hetero. met. proc.	0.0112	-0.0179	0.0185	-0.0974	0.0345	-0.3287	0.0588	-1.5213	0.0272
Protein catabolic proc.	0.0335	-0.4435	0.0185	-0.0974	0	0	0.0735	-2.458	0.0272
Meiosis	0.0168	-0.0647	0.0648	-1.624	0.0517	-0.7063	0.0588	-1.5785	0.0265
Cytoskeleton org.	0.0503	-1.3479	0.0185	-0.1059	0.0862	-1.766	0.0588	-1.598	0.0263
Cofactor met. proc.	0.0168	-0.0751	0.0185	-0.1152	0.0517	-0.7443	0.0368	-0.5851	0.0254
Ribosome biogen.	0.1341	-10.8591	0.0278	-0.2926	0	0	0.0147	-0.0664	0.025
Sporulation	0.0279	-0.3475	0.0278	-0.3031	0.0172	-0.1191	0.0368	-0.6359	0.0245
Cell wall org.	0.0279	-0.3878	0.0093	-0.0339	0.0345	-0.4109	0.0147	-0.082	0.0234
Homeostasis	0.0112	-0.0388	0.0093	-0.0386	0	0	0.0147	-0.0936	0.0223
Conjugation	0.0335	-0.7959	0.0556	-1.6443	0.0345	-0.4611	0.0221	-0.2596	0.0205
Respiration	0.0391	-1.5384	0.0185	-0.2645	0.0517	-1.1385	0.0294	-0.7133	0.0167
Cytokinesis	0.0335	-1.1562	0.0185	-0.2764	0.069	-1.8245	0.0441	-1.6157	0.0163
Chromosome seg.	0.0112	-0.122	0.0278	-0.6615	0.0345	-0.676	0.0147	-0.2201	0.0149
Protein folding	0.0056	-0.0341	0.0185	-0.3457	0	0	0.0147	-0.2524	0.014
Aromatic met. proc.	0	0	0.0185	-0.3702	0.0172	-0.263	0.0147	-0.2595	0.0134
Peroxisome org.	0.0056	-0.0503	0.0093	-0.1343	0.0517	-1.471	0.0147	-0.2983	0.012
Pseudohyphal growth	0.0223	-0.7761	0	0	0.0172	-0.2996	0	0	0.012
Cell budding	0.0279	-1.2912	0.0185	-0.4573	0.0345	-0.8501	0.0147	-0.3342	0.0114
Vitamin met. proc.	0	0	0.0093	-0.1922	0	0	0	0	0.0094
Vacuole org.	0.0168	-0.7162	0.0093	-0.2179	0.0345	-1.0831	0.0294	-1.6037	0.0085
Transposition	0.0168	-0.7399	0	0	0.0172	-0.4151	0.0221	-0.9945	0.0082
Nucleus org.	0.0056	-0.1369	0.0185	-0.7464	0	0	0.0074	-0.2011	0.0071
Vesicle org.	0.0391	-3.7768	0	0	0.0172	-0.488	0.0221	-1.2108	0.0069

ESI Table S2

Frequencies of GO biological process terms associated with electrically distinct strains. "Freq." refers to the frequency of each category among strains with a particular electrical phenotype (*e.g.* decreased conductivity at 10 MHz); the overall frequency is listed in the right-most column.

Genetic interactions (stringent positive) 4384 / 1974 (E/N)			**Genetic interactions (intermediate positive)** 43004 / 4073 (E/N)			**Genetic interactions (stringent, pos. & neg.)** 47190 / 3917 (E/N)			**Physical interactions (Krogan *et al*., Table S8)** 14317 / 3672 (E/N)		
(E / N)	Dec. σ	Inc. σ	(E / N)	Dec. σ	Inc. σ	(E / N)	Dec. σ	Inc. σ	(E / N)	Dec. σ	Inc. σ
300 kHz	3 / 28	21 / 64	300 kHz	15 / 45	107 / 97	300 kHz	21 / 44	90 / 95	300 kHz	4 / 36	17 / 92
10 MHz	21 / 74	3 / 49	10 MHz	157 / 98	23 / 88	10 MHz	190 / 96	27 / 83	10 MHz	31 / 103	2 / 65
P-values	Dec. σ	Inc. σ	P-values	Dec. σ	Inc. σ	P-values	Dec. σ	Inc. σ	P-values	Dec. σ	Inc. σ
300 kHz	0.0548	1.34E-08	300 kHz	2.84E-04	~0	300 kHz	7.49E-07	~0	300 kHz	0.156	9.90E-03
10 MHz	1.67E-06	0.4937	10 MHz	~0	0.2676	10 MHz	~0	0.1104	10 MHz	7.49E-07	0.9349
Expected	Dec. σ	Inc. σ	Expected	Dec. σ	Inc. σ	Expected	Dec. σ	Inc. σ	Expected	Dec. σ	Inc. σ
300 kHz	0.85	4.5	300 kHz	5.1	24.1	300 kHz	5.8	27.3	300 kHz	1.3	8.9
10 MHz	6.1	2.6	10 MHz	24.6	19.9	10 MHz	27.9	20.9	10 MHz	11.1	4.4

ESI Table S3

Functional and protein interactions among electrically distinct strains. For different thresholds of genetic interactions (stringent positive, intermediate positive, and stringent positive & negative), the number of edges (E) and nodes (N) in networks consisting of strains with similar electrical properties is given ("Dec. σ" refers to strains with decreased conductivity, "Inc. σ" refers to strains with increased conductivity), along with the significance level (*P*-value) that the number of edges exceeds the expected number (given in the bottom row).

ESI Dataset S1 (separate file)

Electrical properties of strains at a frequency of 300 kHz. The first two columns give the systematic name and standard name of the deleted gene. Columns 3 and 4 give the log ratio (equation 1) calculated for each strain in two independent experiments, with columns 5 and 6 giving the average and standard deviation of these values. Column 7 provides the inferred average effective conductivity for each strain (units of $\Omega^{-1}m^{-1}$), and column 8 provides the approximate range of conductivities each strain covers (units of $\Omega^{-1}m^{-1}$).

ESI Dataset S2 (separate file)

Electrical properties of strains at a frequency of 10MHz. The first two columns give the systematic name and standard name of the deleted gene. Columns 3 and 4 give the log ratio (equation 1) calculated for each strain in two independent experiments, with columns 5 and 6 giving the average and standard deviation of these values. Column 7 provides the inferred average effective conductivity for each strain (units of $\Omega^{-1}m^{-1}$), and column 8 provides the approximate range of conductivities each strain covers (units of $\Omega^{-1}m^{-1}$).

ESI Dataset S3 (separate file)

Genes associated with distinct electrical properties and significantly enriched GO Biological Process terms. Enriched categories are chosen using a *P*-value cutoff of 0.001 (applying the Bonferroni correction with an alpha value of ~0.05) based on the frequencies listed in Table S2.